Quantum Device Lab
Prof. Dr. Andreas Wallraff
ETH Zürich

Semesterarbeit

Design of microwave beam splitters for photon correlation measurements

Tobias Frey

Mentor:
Dr. Peter Leek

Abstract

For Hanbury Brown and Twiss correlation measurements, which use the signal intensities of the measured waves instead of its amplitudes, beam splitters are necessary. They divide the incoming beam intensity into two beams of equal power. In the two outcoming branches the beam intensities are measured with two photo detectors. Using the correlation of the measured beam intensities, Hanbury Brown and Twiss were able to measure the angular size of an astronomical radio source or a star.
In circuit QED beam splitters are estimated to be a useful tool to perform quantum computing. One possible application for microwave beam splitters would be to a realize an experiment which allows to create entangled states. Entanglement exists only in quantum mechanics and plays a key role in many of the most interesting applications of quantum computation, e.g. in superdense coding.
In this project the task was to search for different types of beam splitters in the literature and to investigate which of the different designs is most suitable to have the possibility to perform correlation experiments with microwave photons. There are two important criteria which the beam splitters had to fulfill in the investigation. The first necessity is that the incoming beam is equally divided to the output ports. The second condition for performing correlation measurements especially with single photons is that the beam splitters have as low loss as possible.
The 90° phase shift hybrid was chosen because it can be operated in the superconducting regime which is necessary to reduce the loss of photons. In addition a coupling of -3 dB can be obtained with a 90° phase shift hybrid and still it has a rather simple geometric structure which is easy to scale. Therefore the 90° phase shift hybrid can be realized on printed circuit boards as well as on smaller length scales on an integrated microchip.
In a first step microstrip technology was used on printed circuit boards (PCB) to test the realization of this type of a beam splitter. The second version was realized using coplanar waveguide technology in order to minimize the size of the circuit. To have as little loss as possible a design working with niobium in the superconducting regime was created. For the design process simulations were undertaken using microwave office. This simulation tool offers the possibility to perform simulations of microwave circuits which are either component based or directly defined by the geometry of the transmission lines and the used substrate for the realization. The performance of the design was tested utilizing a network analyzer. The outcome of the simulations and the measured results were compared and interpreted.
For the microstrip version the measured result showed the characteristic behavior predicted by the corresponding simulations of the circuit. Here some impedance matching problems with the connectors of the board occurred which caused loss and some fast oscillations in the frequency response of the circuit. Initially the measured data of the coplanar waveguide realization were far from the simulation results. Possible reasons might be some problems in the fabrication process of the samples as well as with the proper grounding of parts of the sample. Further measurements of the superconducting samples are still in progress.

Contents

1 Introduction

In 1956, Hanbury Brown and Twiss presented the possibility to measure the angular sizes of an astronomical radio source or a star by the use of correlation measurements. The method was new, because they used the correlations of signal intensities, rather than amplitudes, in independent detectors [1]. In general, correlations are used to investigate the connection between two quantities, here it gives the relation between two electromagnetic waves. A more detailed discussion of the meaning of correlations and the different types of correlation measurements that exist will be given in section 2.1. Using correlations of signal intensities it was also possible to show the bunching of photons in coherent light beams [2].
A number of experiments have been performed in the field of quantum optics using Hanbury Brown and Twiss correlations, e.g. Lounis and Moerner used Hanbury Brown and Twiss correlations to prove that they had a single photon source [3]. But also in particle physics this type of interferometry is used to probe high energy particles [4].
In order to perform Hanbury Brown and Twiss correlation measurements beam splitters are needed which divide the incoming beam intensity into two beams of equal power and measure it in the two outcoming branches with two photodetectors.
Working with photons is not only possible in the visible range of light but also at lower frequencies e.g. with microwave photons. In 2006 J. Gabelli used GHz photons to investigate the microwave photon statistics in quantum systems using Hanbury- Brown and Twiss correlation in his PhD thesis [5].
For correlation measurements with microwave photons, especially for those using a single photon, beam splitters with little loss are crucial for the processing of the beam. Having such a beam splitter it would be possible to show the indivisibility of microwave photons. An other suggestion for an experiment using two microwave beam splitters would be to build a Mach-Zehnder interferometer. Experiments on single photon correlations could then be carried out in the microwave regime. A superconducting qubit could be build in one of the arms in order to perform the phase shift needed to influence the interference of the two signals at the output. But there a more possibilities to think of when using beam splitters as a tool for basic microwave photon quantum optics experiments and quantum computation.
The aim of this Semesterarbeit was to design and implement a 50/50 beam splitter working with GHz photons in a low loss superconducting circuit. Therefore, different types of realization possibilities of beam splitters were investigated. For the most suitable beam splitter analytical calculations were done to understand the basic properties of the circuit. The implementation of the design for this beam splitter was realized and tested on a printed circuit board, PCB, to measure its behavior at room temperature. Two types of versions were realized on a PCB. In one case microstrip technology was used to fabricate the sample, in the

other case the beam splitter was implemented in coplanar waveguide technology. With the coplanar waveguide technology one has the possibility to make the device smaller by decreasing the size of the gap between the center conductor and the ground plane and at the same time maintaining the same impedance. In either case simulations were undertaken before the production of the devices in order to get the characteristic behavior of the beam splitter. In addition a version fabricated on a niobium silicon wafer to measure it in the superconducting phase of niobium was realized. Designs for different operating frequencies were developed and again simulations were undertaken to study the sample's characteristics.
The superconducting designs were put on a optical lithographic mask and later fabricated in the clean room of the ETH by Peter Leek. The development process of the PCB samples could be completely realized in our own lab by myself and so the production took less time. That's why these samples were suitable for testing purposes, even if they are not superconducting and therefore should have more loss. Due to the the demand of little loss and the ability to implement the design on a small chip the final version is designed for working in the superconducting regime.

2 Theory

In order to perform correlations measurements in one's experiment it is important to understand what correlation actually means in the context of electromagnetic waves. Therefore in the following a more detailed explanation is given.

2.1 Correlation

The concept of correlations is used in the context of electromagnetic waves to describe the coherence of a source emitting photons. Electromagnetic waves are called coherent if they have a steady relation of their phases. The phase of an electromagnetic wave depends on time and on space. Therefore we have coherence in space and coherence in time. Knowing the degree of coherence of the system one knows how far the phase of the electromagnetic wave in space and time can be predicted. Having a high degree of coherence is important to be able to perform interference experiments. Interference is the coherent superposition of electromagnetic waves. Two extreme cases occur, either the amplitudes of the waves add up, called constructive interference, or are subtracted from each other, which is referred to as destructive interference. Whether we have destructive or constructive interference depends on the phase difference between the waves. The interference patterns can be observed e.g. on a screen which is held into the photon beam.
If the waves are not coherent the phase between the waves is changing arbitrarily in time and space. Adding up the instantaneous amplitudes of the different waves, their phase relation is changing arbitrarily and therefore no steady interference pattern can be observed on a screen [6] and chapter 2.5 in [7].
An example for a perfect coherent wave is the plane wave, here the equation for the electric field distribution is given,

$$\overrightarrow{E}(\overrightarrow{x}, t) = \overrightarrow{E_0} \cdot e^{i(\overrightarrow{k}\cdot\overrightarrow{x} - \omega\cdot t)} \tag{2.1}$$

where $\overrightarrow{k}$ defines the wave vector and ω the angular frequency. As this wave is perfectly coherent in time and space if we know the phase at one point we can calculate it at each other point in space and time [8].
One can regard different types of orders of coherence functions in order to characterize the coherence of random electromagnetic waves. For random light which is also an electromagnetic wave, which arises e.g. because of unpredictable fluctuations of the light source. The reason for this might be that the light is a superposition of a large number of atoms which radiate independently at different frequencies and phases. Because of the randomness, statistical averages have to be used for classifying the light. With the help of the concept of

statistical averages it is possible to define a number of nonrandom measures. These measures allow to classify the wave as coherent, incoherent or partially coherent [7].

In general for random complex functions $V(\overrightarrow{x}, t)$ expectations values of the form (2.2) are useful to characterize a physical system.

$$\Gamma(t_1, \overrightarrow{x_1}, ..., t_r, \overrightarrow{x_r}, t_{r+1}, \overrightarrow{x_{r+1}}, ..., t_n, \overrightarrow{x_n}) =< V(t_1, \overrightarrow{x_1}) \cdot ... V(t_r, \overrightarrow{x_r}) \cdot V^*(t_r + 1, \overrightarrow{x_{r+1}}) \cdot ... V^*(t_n, \overrightarrow{x_n}) > \tag{2.2}$$

where $< . >$ denotes that the expectation value is used and the * refers to the complex conjugate of the function. This function is called *generalized correlation function*. In a short notation it can be written as:

$$\Gamma_{1,...,n}(t_1, ..., t_n) =< V_1(t_1) \cdot .... \cdot V_r(t_r) \cdot V^*_{r+1}(t_{r+1}) \cdot ... \cdot V^*_n(t_n) > . \tag{2.3}$$

A important special case is the *correlation function* which is defined as:

$$\gamma_{12} = \frac{\Gamma_{12}(t + \tau, t)}{(\Gamma_{11}(t + \tau))^{1/2} (\Gamma_{22}(t))^{1/2}} \tag{2.4}$$

where the following definitions are used: $\Gamma_{12}(t + \tau, t) =< V_1(t + \tau) V^*_2(t) >$
and $\Gamma_{11}(t, t) =< V_1(t) V^*_1(t) >$. Therefore it follows that the relation between the two functions $V_1(t)$ and $V_2(t)$ is investigated by the correlation functions, see chapter 12 in [9].
In the following we focus on electromagnetic waves where with the help of correlation functions the coherence can be defined. In this context the correlation functions are referred to as coherence functions [7] in the literature.

2.1.1 First order coherence function

The first order coherence function takes the correlations between the amplitudes into account. An arbitrary wave can be described by its complex wave function $U(\overrightarrow{r}, t)$. In the case of a plane wave $U(\overrightarrow{r}, t)$ has the form:

$$U(\overrightarrow{r}, t) = U(\overrightarrow{r}) \cdot e^{-i\omega t} \tag{2.5}$$

where ω is the angular frequency.
The intensity of a wave is defined as $I(\overrightarrow{r}, t) = |U(\overrightarrow{r}, t)|^2$. In the case of random electromagnetic waves the quantity $U(\overrightarrow{r}, t)$ is a random function of position and time and is referred to as random or instantaneous intensity. The average intensity is defined as

$$I(\overrightarrow{r}, t) =< |U(\overrightarrow{r}, t)|^2 > \tag{2.6}$$

where $< . >$ is the ensemble average over many realizations of the random function. Each wave of the ensemble is reproduced under the same conditions each time but yields a different wave function.

The mutual coherence function is defined as:

$$G(\overrightarrow{r_1}, \overrightarrow{r_2}, \tau) =< U^*(\overrightarrow{r_1}, t) \cdot U(\overrightarrow{r_2}, t+\tau) > \tag{2.7}$$

where r_1 and r_2 are two points in space and τ is the time delay between the measurements. In a normalized form Eq. (2.7) can be written as:

$$g(\overrightarrow{r_1}, \overrightarrow{r_2}, \tau) = \frac{G(\overrightarrow{r_1}, \overrightarrow{r_2}, \tau)}{(I(\overrightarrow{r_1}) \cdot I(\overrightarrow{r_2}))^{\frac{1}{2}}} \tag{2.8}$$

This equation is called the complex degree of coherence. Its absolute value ranges between

$$0 \leq |g(\overrightarrow{r_1}, \overrightarrow{r_2}, \tau)| \leq 1. \tag{2.9}$$

It measures the degree of correlation of the amplitudes between the fluctuations r_1 and r_2 at time τ later. When $U^*(\overrightarrow{r_1}, t)$ and $U(\overrightarrow{r_2}, t+\tau)$ vary independently and have random phases, meaning the probability for each phase configuration between 0 and 2π is equal. The product in the numerator in Eq. (2.7) gives zero and the waves at this point are called uncorrelated. If Eq. (2.9) is equal to 1, the waves are fully correlated at this point. If one sets τ to zero the spatial coherence can be investigated. Young's double slit experience is a famous example for measuring spatial coherence. If $r_1 = r_2$ and $\tau \neq 0$ the temporal coherence can be determined, also see chapter 10 in [7]

2.1.2 Higher order coherence functions

Experiments using first order coherence can be used to determine the degree of coherence. But one is not able to give a statement about the statistical properties of the electromagnetic wave with first order coherence functions. It's not possible to distinguish between states of electromagnetic waves with identical spectral distribution but with a rather different distribution of photon numbers. The idea of Hanbury Brown and Twiss was to use the intensities of the waves in a correlation experiment instead of the phases of the electromagnetic waves. During the coherence time when the phases are correlated the intensities are correlated as well. Therefore it's possible to obtain the information on the statistics of the electromagnetic waves by counting the photons.
The number of coincident counts is proportional to the ensemble average:

$$C(t, t+\tau) =< I(t)I(t+\tau) > \tag{2.10}$$

where $I(t)$ and $I(t+\tau)$ are the instantaneous intensities. In analogy to the first order coherence function the second order coherence function is defined as:

$$g_2(r_1, r_2, \tau) = \frac{< I(r_1, t)I(r_2, t+\tau) >}{< I(r_1) >< I(r_2) >} = \frac{< E^*(r_1, t)E^*(r_2, t+\tau)E(r_2, t+\tau)E(r_1, t) >}{< |E(r_1)|^2 >< |E(r_2)|^2 >} \tag{2.11}$$

The coherence is defined in the same manner as for the first order coherence. If $|g_1(r_1, r_2, \tau)| = 1$ and $g_2(r_1, r_2, \tau) = 1$ it is said that there is coherence to second order. The function g_1 denotes the first order coherence function and g_2 stands for second order coherence function, for a more detailed discussion of this topic see chapter 5 in [10].
Hanbury Brown and Twiss found in their experiment, that for zero time delay the detection rate was double compared to the case when they took a long time delay. Their conclusion was that photons arrive in pairs [2]. This effect is called the *photon bunching effect or Hanbury Brown and Twiss effect*. It is also possible to measure the coherence time by counting the coincident photons depending on the delay time τ between the measurements, see chapter 3 in [11]. In circuit QED using a microwave beam splitter experiments e.g. investigating the statistics of microwave photons are possible to perform. In ([5]) the statistics of coherent as well as thermal photons were investigated.

2.2 Some network analysis principles

In this thesis network analysis techniques were used to understand and to analyze the working principle of microwave circuits as well as for the creation of the different designs. In the following an introduction to the concept of the scattering matrix and the transmission (ABCD) matrices, which are both parts of network analysis principles, will be given. These two principles for analyzing microwave circuits are used to understand the theory of the different types of beam splitters, see chapter 3, and allow us to compare our measurement results of the beam splitter with predicted results obtained by calculations. The created designs will be presented and discussed in chapter 5.

In general circuit analysis concepts can be used in many cases to understand microwave circuits. In principle one could always solve Maxwell's equations but in most cases this is rather difficult. As the solution of the Maxwell's equations for a given problem is complete it gives the electric and magnetic field everywhere in space. But often one just needs some type of *global quantity*, e.g. voltage or current at some ports, which can be obtained by using microwave analysis. This analysis technique is easier to handle than the Maxwell's equations whose solution contains more information than required. Another advantage of microwave circuit analysis is that it is easy to modify. For example a system can be analyzed as several components and the response of the complete system is obtained by putting the response of the individual components together which is possible due to the linearity of the response. In general the starting point in using microwave network analysis is that one first regards Maxwell's equations for some canonical problems and tries to solve them. Having the corresponding solutions one tries to obtain quantities which allow to relate them directly to the circuit, e.g. the propagation constant or the characteristic impedance of the transmission line. By these means one has the possibility to treat e.g. the transmission line as a distributed component which can be characterized by its length, propagation constant and characteristic impedance. The concept of distributed components gives rise to the possibility to interconnect various components and

use circuit analysis concepts of the individual parts of the design to obtain the behavior of the entire system e.g. reflection and transmission coefficients. For completeness it should be mentioned that in some cases circuit analysis concepts are an oversimplification and the Maxwell equations have to be used to get a correct result, however this is not the case for the circuit we are analyzing here, page 161 ff in [12].

2.2.1 The scattering matrix

The concept of the scattering matrix is to deal with the ideas of incident, reflected and transmitted waves of a N-port network and provides a complete description of the circuit. The scattering matrix describes the relation between the voltages of the incident waves with propagation in the direction of the ports to the voltage of the corresponding reflected waves. For an N-port network it is defined as:

$$\begin{pmatrix} V_1^- \\ V_2^- \\ . \\ . \\ . \\ V_N^- \end{pmatrix} = \begin{pmatrix} S_{11} & S_{12} & . & . & . & S_{1N} \\ S_{21} & S_{22} & . & . & . & S_{2N} \\ . & & & & & \\ . & & & & & \\ . & & & & & \\ S_{N1} & S_{N2} & . & . & . & S_{NN} \end{pmatrix} \begin{pmatrix} V_1^+ \\ V_2^+ \\ . \\ . \\ . \\ V_N^+ \end{pmatrix}. \tag{2.12}$$

or in a short notation:

$$[V^-] = [S][V^+]. \tag{2.13}$$

Here V_j^+ is the voltage amplitude of the incident wave on the j^{th} port and V_i^- is the voltage amplitude of the reflected wave from the i^{th} port. A specific element of the scattering matrix $[S]$ can be calculated as:

$$S_{ij} = \frac{V_i^-}{V_j^+}|_{V_k^+=0, \forall k \neq j}. \tag{2.14}$$

This means S_{ij} is obtained by applying an incident wave with amplitude V_j^+ on port j and by measuring the emerging amplitude voltage V_i^- on the i^{th} port. All the other ports expect the j^{th} port a terminated with a matched impedance in order to avoid unwanted reflections. Terminating a port with a matched load means for the mathematics to set the corresponding voltages to zero. Hence the S_{ii} coefficient is the reflection obtained when all other ports have matched impedance as termination. The coefficient S_{ij} describes the transmission that is taking place from port j to port i, again if all other ports are terminated with matched loads. The calculation of the S-matrix is done using network analysis techniques but the individual parameters can also be directly obtained by using a network analyzer to measure them. In our lab we have such a network analyzer with which we obtained the S matrix elements of our circuits. In addition the S-parameters can be converted to other matrix parameters e.g. the ABCD matrix parameters.

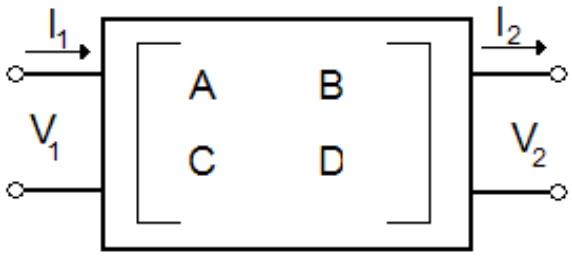

Fig. 2.1: Direction of the currents and voltages used in the definition of ABCD matrix

2.2.2 ABCD matrix

In practice many microwave circuits consist of only two ports or can be divided into a circuit consisting of only two port components. In this case it is useful to define the $ABCD$ matrix which contains two lines and two columns. The matrix is defined as in the following equations:

$$V_1 = A \cdot V_2 + B \cdot I_2 \tag{2.15}$$

$$I_1 = C \cdot V_2 + D \cdot I_2 \tag{2.16}$$

or in the matrix form:

$$\begin{pmatrix} V_1 \\ I_1 \end{pmatrix} = \begin{pmatrix} A & B \\ C & D \end{pmatrix} \begin{pmatrix} V_2 \\ I_2 \end{pmatrix}. \tag{2.17}$$

Here the convention is chosen that I_2 flows out of port 2 and I_2 is therefore the same current that flows into the next two port network, if the two are interconnected. The definitions are also shown in figure 2.1. If two circuits are interconnected with each other one only has to multiply the two $ABCD$ matrices in the same order as they are arranged in the circuit to obtain the matrix of the complete network. For the $ABCD$ matrices there exists a library for often used two port circuits.
The procedure is the following if one has to calculate the $ABCD$ matrix for a given microwave circuit: At first one tries to subdivide the circuit into components so that the whole circuit can be build up as a network of two port networks. After that one tries to part the remaining two port circuits into those circuits that are already known in the library for $ABCD$ matrices. The matrix for the whole circuit can be obtained by first multiplying the different $ABCD$ matrix to obtain the $ABCD$ matrices for the combined two port systems and afterwards adding the calculated two port matrices. The way they are added is given by the circuit diagram of the two component network which was created when the complete circuit was divided into a network of two port components. This procedure is not always possible as it depends on the symmetry of the circuit. The $ABCD$ matrix can be converted to S-parameters, see equations 3.9, 3.10, page 174 ff in [12]

3 Survey of beam splitter designs

There are several possibilities to realize a beam splitter for microwave photons. Most of the beam splitters were invented and characterized in the 1940s at the MIT Radiation Laboratory using coaxial probes. Mostly in 1960s they were reinvented using microstrip technology.
In the following we will discuss the most used possibilities for realizing a beam splitters. There exist two principle ways of realizing a beam splitter. One version has only three ports and has the form of a T - junction. The other version is a four port network and examples are the 90° hybrid and coupled line couplers.
The criteria the beam splitters had to fulfill in order to be suitable for single photon correlation experiments are the following. A design of the beam splitter version must be realizable which divides the input power equally to the two output ports. In addition it has to be possible to operate the beam splitter in the superconducting regime in order to minimize the loss as much as possible. The third criterion is that the design is scalable. This means that having a design working on PCB board and then downsizing the layout of the circuit in order to place the beam splitter on a chip no complications due to geometry and space should occur concerning e.g. the grounding of parts of the circuit with bond wires.

3.1 Wilkinson divider

In general T- junctions, three port networks, can't be lossless, reciprocal and matched at each port, chapter 7.1 in [12]. Having a lossless circuit means that no electric power is converted into heat within the circuit. A network is known to be reciprocal if it is passive and contains only isotropic materials and matching refers to equal impedances. They have the same value which is called matched and so therefore no reflections of the signal due to an impedance mismatch occurs. As T-junctions can fulfill all these criteria, a resistor is added in the design of the Wilkinson splitter. A microstrip version of a Wilkinson beam splitter is shown in Fig. 3.1.

The signal coming through port 1 is split up and the same power can be measured at the two output ports 2 and 3. There's no phase shift between the two output ports. Each of the ends of the isolation resistor is at the same potential, therefore no current flows through the resistor and the resistor is decoupled from the input signal. Adding up the two output port impedances in parallel yields the input impedance. Labeling the input impedance with Z_0 it follows that the resistor must have the value $2 \cdot Z_0$. The transmission lines must have a length of $\frac{\lambda}{4}$ and their characteristic impedance must be $\frac{Z_0}{\sqrt{2}}$ in order to have a matched input when ports 2 and 3 are terminated in Z_0.

A more detailed description and the actual calculations can be found in chapter 7.3 in reference [12].
The problem with the Wilkinson splitter for our application is that in the superconducting regime of the transmission lines the resistor between the transmission lines must stay normal which experimentally difficult to handle.

3.2 Coupled lines

The coupled line realization of a beam splitter belongs to the group of the four port networks. The functional principle is that the lines are so close to each other that energy from one line passes to the other. Figure 3.2 shows the circuit diagram of a coupled line splitter. The signal comes in through port 1, port 2 is for the transmission, on port 3 the signal due to coupling of the lines should be measured. Port 4 is called isolated which means that no power can be measured there. The coupling strength is described by a coupling constant C which is defined as:

$$C = \frac{Z_{0e} - Z_{0o}}{Z_{0e} + Z_{0o}} \tag{3.1}$$

where Z_{0e} stands for the impedance of the even mode excitation and Z_{0o} describes the impedance of the odd mode excitation, see section 7.6 in [12]. Depending on the length of the parallel lines the voltage is transferred between the two lines, which can be seen in figure 3.3. Here θ describes the length of the lines and 2π corresponds to the wavelength λ.
The different impedances and therefore also the coupling strength depends strongly on the gap between the lines, the smaller the gap the larger the coupling strength. The coupling line couplers are suitable for weak couplings as for strong coupling the gaps have to be so small and are therefore unpractical [12]. Nevertheless Chen et.al from the Institute of Electronics in Taiwan managed to realize a $-3\,\mathrm{dB}$ coupler with coupled lines using microstrip technology. Their required line width was 309 μm and the interline spacing 4 μm. Their good result is only obtained due to the smaller coupling gap and no extra tricks had to be used [13].
The problem using this technology is the scaling. In order to have a $-3\,\mathrm{dB}$ coupler the small

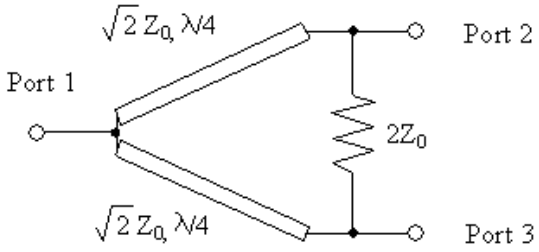

Fig. 3.1: Circuit diagram of a Wilkinson beamsplitter, Z_0 stands for the impedance and λ is the wavelength of the design frequency

gap has to be realized. As our first experiments should be performed on a PC board where we don't have a resolution in the fabrication process up to 4 μm we didn't take this type of beam splitter. The big advantage of realizing your circuit on PC board is that the fabrication process is much faster than the one for the optical lithography used in the FIRST lab of the ETH. Therefore in order to get some understanding of the problems that might occur using beam splitters, a type of beam splitter was searched for which is easy to build a scalable model of.
In order to build $-3\,\mathrm{dB}$ beam splitter with coupled lines Lange couplers were invented. A picture of a Lange coupler is shown in Fig. 3.4. A Lange coupler has more lines being parallel to each other so the coupling is stronger. The problem with the Lange coupler is that the bonding becomes rather complicated especially when the lines get smaller, the scaling is again a problem. Therefore we didn't realize one of this type of beam splitter.

3.3 90° phase shift hybrid

Another possible realization of a beam splitter is the 90° phase shift hybrid. It consists of four transmission lines which form a rectangle see Fig. 3.5. Pairs of opposite lines have the same impedance, one pair has an impedance of Z_0 and the other has an impedance of $\frac{Z_0}{\sqrt{2}}$. The hybrid fulfills its task to split an incoming microwave in two waves with the same power only at a certain frequency. This frequency is called the design frequency. The four transmission lines have an electrical length of $\frac{\lambda}{4}$. As this beam splitter just depends on the impedances of the different transmission lines it is easy to scale and can be realized on PC boards and on smaller length scales for a chip design as well. We therefore decided to fabricate this type of beam splitter. In the following sections it will be explained how an hybrid works and why the lines have to be $\frac{\lambda}{4}$ long and why the hybrid therefore only splits the incoming beam equally at a certain design frequency.

To begin with the analysis of a hybrid one must consider the characteristics of transmission lines. For a lossless transmission line the input impedance is given by 3.2:

$$Z_{in} = Z_0 \frac{Z_L + iZ_0 \tan(\beta l)}{Z_0 + iZ_L \tan(\beta l)}, \tag{3.2}$$

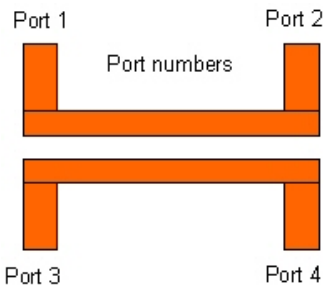

Fig. 3.2: Circuit diagram of a coupled line

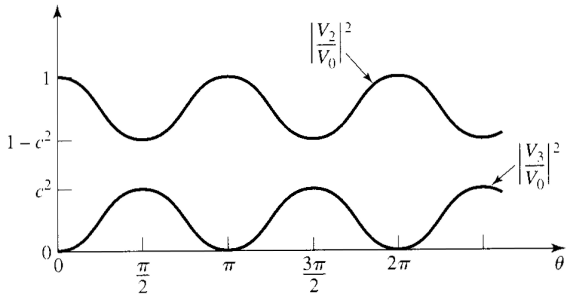

Fig. 3.3: Coupling of the lines, on the x-axis θ describes the length of the lines and 2π corresponds to the wavelength λ which is plotted versus the square of the absolute value of the voltages, normalized to the input voltages, at the output ports 2 and 3

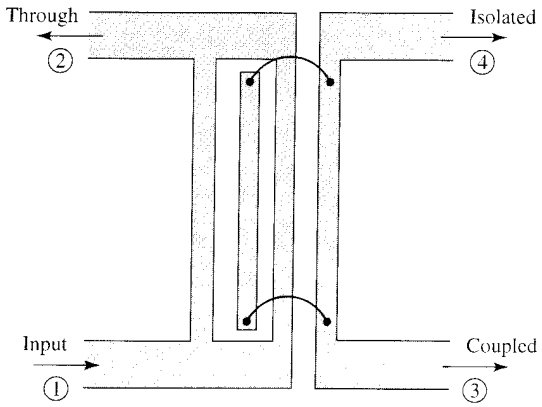

Fig. 3.4: Circuit diagram of a Lange coupler

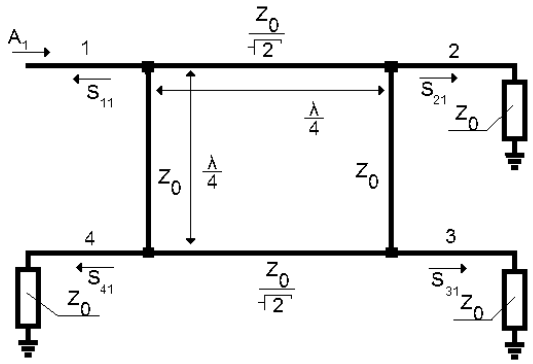

Fig. 3.5: Circuit diagram of a 90° hybrid. Numbers 1,2,3,4 name the ports, A_1 is the input amplitude, S_{ij} are the S-parameters of the individual ports, Z_0 stands for the impedance and λ is the wavelength of the design frequency.

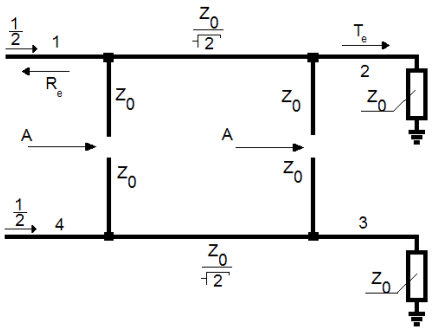

Fig. 3.6: Even mode of the 90° hybrid. Numbers 1,2,3,4 name the ports, A_1 in the input amplitude, S_{ij} are the S-parameters of the individual ports, Z_0 stands for the impedance and λ is the wavelength of the design frequency.

where l denotes the length of the transmission line and β is the wave vector. For a short-circuited ($Z_L = 0$) line one obtains from Eq. (3.2).

$$Z_{in} = iZ_0 \tan(\beta l). \tag{3.3}$$

For an open circuited line ($Z_L = \infty$) Eq. (3.2) can be written as:

$$Z_{in} = -iZ_0 \cot(\beta l). \tag{3.4}$$

As already mentioned in section 2.2 it is possible to characterize the whole behavior of a 2 port microwave circuit if the parameters A, B, C, D are known.
The ABCD- parameters for a parallel circuit are the following: $A = 1$, $B = 0$, $C = Y$, $D = 1$. For an arbitrary transmission line the ABCD parameters are: $A = \cos(\beta l), B = iZ_0 \sin(\beta l)), C = iY_0 \sin(\beta l), D = \cos(\beta l)$, page 185 in [12].
To analyze the properties of the 90° hybrid, symmetry properties of the circuit can be used. As shown in the Figs. 3.6 and 3.7 the circuit can be simplified in even and odd mode excitations. The amplitudes of the input signal are either $\frac{1}{2}$ at port 1 and 4 in the even mode or $\frac{1}{2}$ at port 1 and $-\frac{1}{2}$ at port 4 in the odd mode excitation. Combining this two figures 3.6, 3.7 one obtains figure 3.5 back.Due to the possibility to divide the circuits one gets two decoupled two-port networks that are more simple to analyze.

3.3.1 Even mode excitation

In the even mode, the circuit can be split in the middle at point A, see Fig. 3.6, and each part consists of two open circuited lines and one transmission line. The ABCD matrix of each component can be calculated using the definitions for Z and the ABCD parameters given in section 3.3. To obtain the matrix of the combined elements the individual matrices must be

multiplied. For the open circuited stubs one obtains the matrices M_{1e} and for the second stub M_{3e}. In this case M_{1e} and M_{3e} are the same because the two stubs have the same geometry and consist of the same material. They are referred to as different so that it would be easy to deal with other circuits where l and β aren't the same for both of them. Different values for l and β occur when effects of asymmetries in the circuit are studied.
Matrix M_{2e} refers to the transmission line between the two open circuited stubs. As this hybrid consists of four $\frac{\lambda}{4}$ transmission lines where λ stand for the wavelength and the circuit 3.5 is divided in the middle, the two stubs have a wavelength of $\frac{\lambda}{8}$. So for l_1, $\frac{\lambda}{8}$ and for l_2, $\frac{\lambda}{4}$ is inserted in Eq. (3.8). The e stands for the even excitation mode whereas for the odd excitation mode an o will be used to refer to.

$$M_{1e}(\beta, l_1, Z) := \begin{pmatrix} 1 & 0 \\ i\frac{1}{Z}\tan(\beta \cdot l_1) & 1 \end{pmatrix}. \tag{3.5}$$

$$M_{2e}(\beta, l_2, Z) := \begin{pmatrix} \cos(\beta \cdot l_2) & i\frac{Z}{\sqrt{2}} sin(\beta \cdot l_2) \\ i\frac{\sqrt{2}}{Z}\sin(\beta \cdot l_2) & cos(\beta l_2) \end{pmatrix}. \tag{3.6}$$

$$M_{3e}(\beta, l_1, Z) := \begin{pmatrix} 1 & 0 \\ i\frac{1}{Z}\tan(\beta \cdot l_1) & 1 \end{pmatrix}. \tag{3.7}$$

Multiplying the three matrices gives the complete ABCD matrix for the even mode circuit.

$$M_{te}(\beta, l_1, l_2, Z) = M_{1e}(\beta, l_1, Z) \cdot M_{2e}(\beta, l_2, Z) \cdot M_{3e}(\beta, l_1, Z). \tag{3.8}$$

In section 2.2 it was shown that a microwave network among others can be either characterized by the S parameters or the ABCD matrices. As the network analyzer we use to investigate the electric properties of our circuits measures the S- parameters in the following the ABCD matrices of the even mode excitation are converted to the corresponding S-parameters. To do this the following formulae were used:

$$S_{11e/o} = \frac{A + \frac{B}{Z_0} - CZ_0 - D}{A + \frac{B}{Z_0} + CZ_0 + D} \tag{3.9}$$

$$S_{21e/o} = \frac{2}{A + \frac{B}{Z_0} + CZ_0 + D} \tag{3.10}$$

The S-parameters for the odd mode are labeled with an o whereas those for the even mode are labeled with an e.

3.3.2 Odd mode excitation

If one considers the odd mode excitation, the circuits can be split in the middle at point A in figure 3.7 again but due to the different input signals each part consists of two short-circuited stubs and a transmission line. Again one uses the ABCD matrix of a parallel circuit and that of a transmission line. Using Eq. (3.3) one gets three matrices for each element of the circuits.

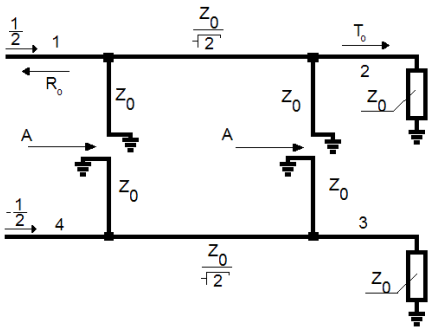

Fig. 3.7: Odd mode of the 90° hybrid. Numbers 1,2,3,4 name the ports, A_1 in the input amplitude, S_{ij} are the S-parameters of the individual ports, Z_0 stands for the impedance and λ is the wavelength of the design frequency.

The matrix of the whole circuit is again obtained by multiplying the different matrices. The three matrices are :

$$M_{1o}(\beta, l_1, Z) := \begin{pmatrix} 1 & 0 \\ -i\frac{1}{Z}\cot(\beta \cdot l_1) & 1 \end{pmatrix}. \tag{3.11}$$

$$M_{2o}(\beta, l_2, Z) := \begin{pmatrix} \cos(\beta \cdot l_2) & i\frac{Z}{\sqrt{2}} sin(\beta \cdot l_2) \\ i\frac{\sqrt{2}}{Z}\sin(\beta \cdot l_2) & cos(\beta l_2) \end{pmatrix}. \tag{3.12}$$

$$M_{3o}(\beta, l_1, Z) := \begin{pmatrix} 1 & 0 \\ -i\frac{1}{Z}\cot(\beta \cdot l_1) & 1 \end{pmatrix}. \tag{3.13}$$

Multiplying the three matrices gives the complete ABCD matrix for the odd mode circuit. For the lengths l_1 and l_2 the same values as in the even mode case are used. Using Eq. (3.9) and (3.10) the corresponding S- parameters can be found.

3.3.3 Combination of even and odd mode excitation

In order to describe the behavior of the complete circuit one has to combine the two excitation modes. From Figs. 3.6 and 3.7 one gets the emerging wave of the complete circuit at each port as a superposition of the odd and even mode excitation. The relations are given by the following four equations.

$$S_{11} = \frac{1}{2}S_{11e} + \frac{1}{2}S_{11o}, \tag{3.14}$$

$$S_{12} = \frac{1}{2}S_{21e} + \frac{1}{2}S_{21o}, \tag{3.15}$$

$$S_{13} = \frac{1}{2}S_{21e} - \frac{1}{2}S_{21o}, \tag{3.16}$$

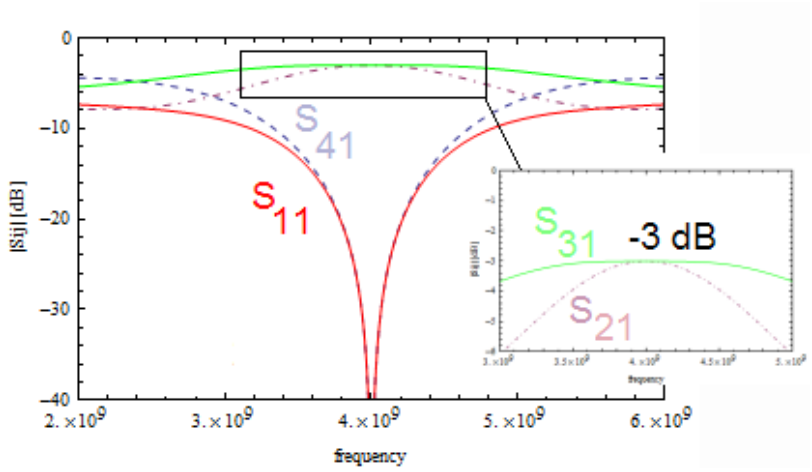

Fig. 3.8: S-parameters in dependence of the applied frequency

$$S_{14} = \frac{1}{2}S_{11e} - \frac{1}{2}S_{11o}. \tag{3.17}$$

The S_{ije} or S_{ijo} parameters are those which were obtained using the Eqs. (3.9) and (3.10). Now one is able to calculate the different S-parameters of the hybrid in dependence of the applied frequency. The different S-parameters in dependence on the applied frequency are shown in Fig. 3.8. The inset in Fig. 3.8 shows the scattering parameters S_{21} and S_{31} in more detail, it can be seen that at 4 GHz which is the design frequency the coupling is exactly $-3\,\mathrm{dB}$ neglecting all types of losses. At the design frequency $S_{11} = 0$, $S_{12} = -\frac{i}{\sqrt{2}}$, $S_{13} = -\frac{1}{\sqrt{2}}$ and $S_{14} = 0$. One says that port one is matched, and port 4 is isolated. At port 2 and 3 one measures half of the input power but between port 1 and 2 one gets a phase shift of -90°, whereas for port 3 we have a phase shift of -180° with respect to port 1. Subtracting the phase difference of port 2 from that of port 3 we obtain a phase shift of 90° between the phases of the 2 port. Therefore this type of beam splitter is called a 90° hybrid. As we have a logarithmic scale in figure 3.8, S_{11} and S_{14} go to infinity and S_{21} and S_{31} have the value of $-3\,\mathrm{dB}$.

4 Implementation

In this chapter the implementation of the beam splitter is treated. For the realization of the transmission lines two technologies were used namely microstrip and coplanar waveguide. Therefore in section 4.1 an introduction to microstrip as well as coplanar waveguide technology is given. At the end of this section the advantages and disadvantages of each technology for the purpose of designing a beam splitter for correlation measurements are discussed. In the proceeding section the way impedances for the different designs were calculated is described. The section about Simulation - Microwave office deals with the properties of the simulation process. The last section in this chapter describes the fabrication process for the normal as well as for the superconducting samples.

4.1 Introduction to microstrip waveguide circuits and coplanar waveguide circuits

Microstrip lines are one of the most used planar transmission line geometries. It consists of a conductor which is on top of a dielectric substrate, figure 4.1 (a). The dielectric is grounded on the other side. Due to the dielectric most field lines are present in the region between the conductor and the ground plane, so there are weaker fields in the air region above the dielectric substrate. In figure 4.1 (b) an example of a possible field distribution of a microstrip transmission line is shown. Microstrip lines can't support pure TEM-waves because the phase velocity in the dielectric is given by $\frac{c}{\sqrt{\varepsilon_r}}$ whereas in air it is simply c, the velocity of light. ε_r is the relative permittivity. TEM-wave is the abbreviation for transverse electromagnetic wave which means that the E-field the B-field and the wave vector k which gives the direction of the wave are perpendicular to each other. So there is no possibility to have a phase match between those parts of the wave in the air and the ones in the substrate for a pure TEM- wave. To get the actual field distribution is quite complicated but there is a good approximation that can be made. This approximation can be done if $d \ll \lambda$ where d is the thickness of the dielectric substrate and λ is the wavelength. In this case one speaks of quasi-TEM waves and uses the same calculations as for pure TEM-waves. So calculations are of course only approximations but in practice one noticed that it works well. The phase velocity v_p and the propagation constant β can therefore be expressed as:

$$v_p = \frac{c}{\sqrt{\varepsilon_e}} \tag{4.1}$$

$$\beta = k_0\sqrt{\varepsilon_e} \tag{4.2}$$

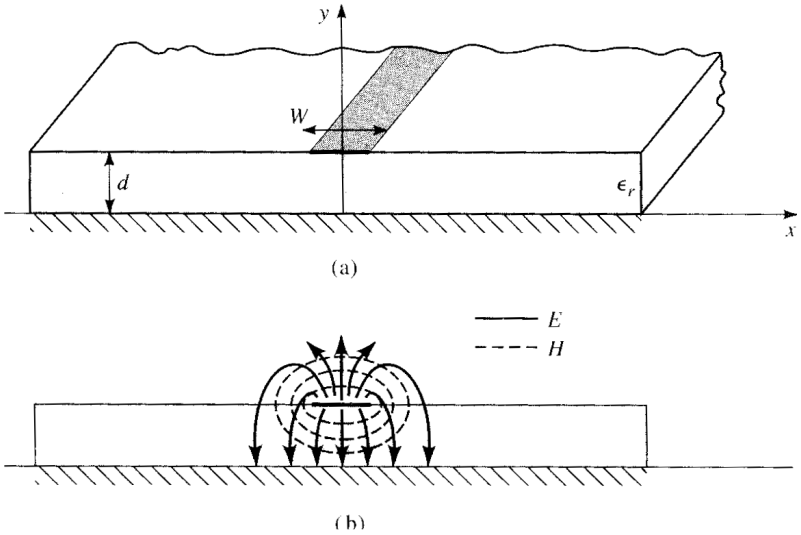

Fig. 4.1: a) Design parameters of a microstrip line, b) field distribution for a transmission line cross section viewed; ε_r is the relative permitivity, W width of the transmission line, d height of the dielectric substrate, E stands for the electric field and H for the magnetic field

ε_e is the effective dielectric constant of the microstrip line. As parts of the field lines lie in the dielectric material and the other part in air, ε_e fulfills the following inequalities:

$$1 < \varepsilon_e < \varepsilon_r \tag{4.3}$$

In addition ε_e depends on the substrate thickness and the conductor width, see page 143ff [12].
Coplanar waveguide, abbr. CPW, which is illustrated in Fig. 4.2, consists of a center strip conductor which is surrounded by two ground planes which are separated by a gap of width W from the center conductor atop a dielectric material and a ground plane on the lower side of the dielectric. A good reference for detailed discussion of coplanar wave guide technology is the book of Simon, see [14].

The main reason why we only used microstrips for one design is that our structure is quite large in this technology and it was therefore not possible to fit it onto a small chip. So we used coplanar waveguide. The main advantage of this technology for our purpose is that the characteristic impedance is determined by the ratio of $\frac{a}{b}$, see chapter 1 in [14]. Therefore size reduction is only limited by the resolution of the lithography. This gave us the possibility to fit our circuit on a chip. As structures get smaller one has higher losses but as our aim was to build a superconducting beam splitter, the loss is not a limiting factor.

4.2 Impedance calculation

For the calculation of the lengths and the widths of the microstrip and the CPW version, TXLine was used. TXLine uses numerical routines for the calculation of the transmission lines,

for more details on the algorithms check: http://web.awrcorp.com/. For the superconducting version it was necessary to use another approach for the calculations of the impedances. This was necessary because TXLine works with numeric algorithms and therefore can't calculate impedances for superconducting transmission lines where the conductivity is infinite. In order to perform these calculations the formulae were taken from Simon's book [14] out of the chapter 3.2, which calculate the impedances for infinite conductivity analytically.

4.3 Simulation - Microwave office

Microwave office is a program which allows us to simulate the behavior of our microwave circuit on different levels of abstraction. Concerning the different levels of abstraction one can simulate a schematic. Here a finite element simulation of the different components in the circuit is performed. The advantage of a schematic is that simulation time is only few minutes and therefore this type of simulation offers a fast way to obtain the circuit's behavior. In our case for the 90° hybrid the disadvantage is that the corners where different geometries of transmission lines are plugged together is idealized as a point like contact and the real geometry of this region taking the width of the transmission lines into account is neglected.
The second type of possibility for performing a simulation is called an EM-structure simulation. Here the circuit is drawn with individual transmission lines in our case in CPW or microwave technology on the dielectric substrate and the whole structure is simulated. For the 90° hybrid this means that the actual geometry of the corners are taken into account and therefore it was possible e.g. to investigate what effect the geometric extent of the transmission lines have especially at the corners of the 90° hybrid where three transmission lines of a different geometry, are plugged together. This problem will be dealt in more detail in chapter 5.
The main disadvantage of an EM structure simulation is the time the simulation needs , e.g. for the non superconducting CPW ones it took up to 5 hours.
An important point to note is that Microwave office takes losses into account when simulating the behavior of a circuit. Due to this reason in the simulations the ideal value of $-3\,\mathrm{dB}$ for

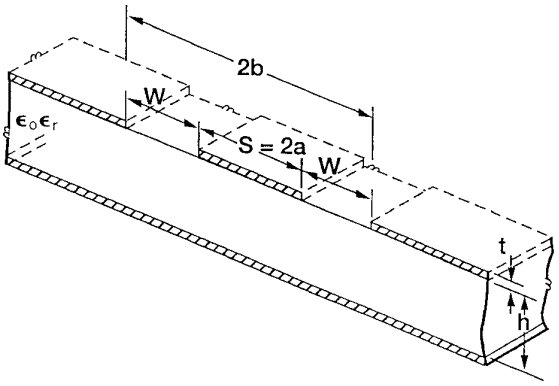

Fig. 4.2: Model of a coplanar waveguide line. W is the width of the gap, S the width of the transmission line, ϵ_r is the relative permitivity, t is the thickness of the conducting material and h the height of the dielectric.

the splitting is not reached but values a little less than $-3\,\mathrm{dB}$. This should be kept in mind when analyzing the simulation results in chapter 5.

4.4 Fabrication of a circuit

After the simulation results agreed with the theoretical analytically calculated results of the 90° hybrid the next step was to fabricate the circuit in order to check whether the real device is working like predicted by the simulation. The beam splitters were designed using a 2D CAD software. The fabrication process was different for the designs realized on a PC-board, see 4.4.1, in contrast to those realized on a chip see 4.4.2.

4.4.1 PCB scale models

The printout of the circuit was transferred to a transparency using photograph techniques. A problem that could occur was that the photo paper was a bit overexposed and therefore the lines on the transparency were a little shiny, later in the fabrication process this causes problems with the optical lithography process. Due to the shiny lines the photo resist is exposed to ultraviolet light were it shouldn't be. In our experience it was therefore better to a take shorter exposure time than measured by the photo-detector.
The next step was the creation of the photo resist layer on the PCB, which had to be as smooth as possible, in order to be able to perform optical lithography later. Having exposed the sample to ultraviolet light and then developed the photo resist the sample was etched. The etching time was difficult to handle because it strongly depended on how fresh the etch was. So it was necessary to check regularly whether the copper was already etched away properly. The last step in the fabrication process was to solder the connectors on and afterwards it was checked with an ohm meter whether an unwanted connection between the ground plane and the transmission line with solder was created.

4.4.2 Superconducting circuits

The superconducting samples were fabricated in the clean room of the ETH by Peter Leek. To do so an optical lithograph mask had to be produced before. After the lithography and the etching which was done similarly as for the PC boards the wafer had to be sawed in order to obtain the individual chips. After that they had to be bonded on a PC-board. The PC board could be mounted in the measuring appliance in order to characterize the chip with the network analyzer. The advantage fabricating the samples in the clean room is that with the optical lithography technique a resolution up to $1\mu m$ can be achieved. Therefore the structures of the beam splitter could be made so small to fit on a chip of 2 mm by 7 mm.

5 Measured data and interpretation of the results

The first section of this chapter deals with the measurement techniques being applied to test the functionality of the beam splitter samples. In the section 5.2 and 5.3 the designs and the outcome of the measurements for the realization of the beam splitters using microstrip and coplanar waveguide technology on a PCB, are presented and discussed. For the superconducting sample the design on the mask and its advantages compared to PCB samples are dealt with in section 5.4.

5.1 Measurement techniques

To test the functionality of the samples the measurements were done using a network analyzer. Measuring high frequency signals the first thing that had to be done was to calibrate the network analyzer for the cables which were used to connect the device with the analyzer in order to take length and impedances of the cables into account.
The functionality test of the samples covered the magnitude of the transmitted and reflected waves as well as the corresponding phases. For the PCB sample the design frequency is 5 GHz, therefore the measurement array was set to range from 4 GHz to 6 GHz. The superconducting samples had to be dipped into liquid helium. As helium has approximately the same dielectric constant, $\epsilon = 1.000070$, as air it is no problem that the sample is now surrounded by helium rather than air. For the superconducting beam splitters three different design frequencies were realized: 7 GHz, 8 GHz and 9 GHz.

5.2 Microstrip version

For each design a simulation of the microwave circuit model was done first, see section 4.3. Like this it could be checked that we didn't make any errors concerning the calculations. Afterwards an em simulation was performed to simulate the circuit under conditions where more effects like e.g. the geometry of the corners are taken into account, see also section 4.3. Comparing the bottom of figure 5.1 which is the result obtained from a schematic simulation, with the top part of this figure obtained from em simulation a difference can be seen. The schematic simulation agrees with the characteristic behavior obtained by analytical calculations. The em structure simulation deviates from these results, as the diagram of S_{21}

and S_{31} is asymmetric with respect to a vertical line at the design frequency of 5 GHz. In addition at the design frequency the beam is not equally split between the two port. S_{21} equals -3,423 dB and S_{31} reads -2,808 dB. For an equal splitting of the incoming waves to the two port both values should be -3 dB. This deviation is due to the fact that the geometry of corners where the different lines are connected to each other aren't idealized as point like contacts anymore like in the schematic simulation but have a certain extension. The structure seen in figure 5.2 was realized to figure out if the simulation gives us some realistic results and to learn the fabrication of the sample. The design frequency was chosen to be 5 GHz, the substrate was RO4350B height 20mil, as the connectors and the cables of network analyzer have an input impedance of 50 Ω, Z_0 was chosen to be 50 Ω. The width of the two 50 Ω lines are 1100 μm, the length 8900 μm, for the $\frac{50}{\sqrt{2}}$ lines a length of 8700 μm and a width of 1900 μm were calculated. The outcome of the measurement is shown in Fig. 5.3. From the measurement results of the microstrip version we could learn that our first sample is working in principle as the graphs of the different S parameters have the characteristic forms as obtained by analytical calculations of the sample's behavior. The bottom part of figure 5.3 is a zoom in into the top part of the same figure which displays the whole measurement array. It shows the transmission to port 2 is around $-4\ dB$ and to port 3 is around $-4\ dB$ as well.
As can be seen the signal has some fast fluctuations on. These fast fluctuations on the signal occurred due to an impedance mismatch caused by the connectors. As we didn't have the connectors for a board of this width, the gaps between the board and the connectors had to be filled with solder. A second problem that emerged is that due to the fact that the connectors hadn't the dimension like the board it was difficult to solder them perpendicular to the board which could cause reflections as well. The phase difference between the output ports is plotted in Fig. 5.4. To obtain this phase shift one measures the phase difference between port 1 and 2 and the difference between 1 and 3. Subtracting these two values from each other the phase difference between the output ports is found. As predicted by the calculations the difference in phase is 90°, see 5.4.
Recapitulatory from this sample we could learn that our circuit works in principle and had a better idea of how to fabricate the sample on a PC board.

5.3 Coplanar waveguide

As the dimension of the microstrip sample is too large to put it on a chip of the size of 2 mm width and 7 mm length and as it's more difficult to bend transmission lines the bigger the width of the lines are the next step was to realize a coplanar waveguide 90° hybrid. With coplanar waveguide technology it is possible to shrink the size of the sample and maintain the same dielectric material and design frequency, see section 4.1. As the conductivity of these samples is finite TXLine could be used to obtain the width and the length of the lines. For a first test of the design schematic as well as EM structure simulations were performed. The results are displayed in figure 5.5. Again two lines were chosen to have 50 Ω, their length is 6400 μm and the value for the width is 700 μm . The other two transmission lines with an impedance of $\frac{50}{\sqrt{2}}$ have a width of 1700 μm and the length of each is 6200 μm. The design frequency is 5 GHz

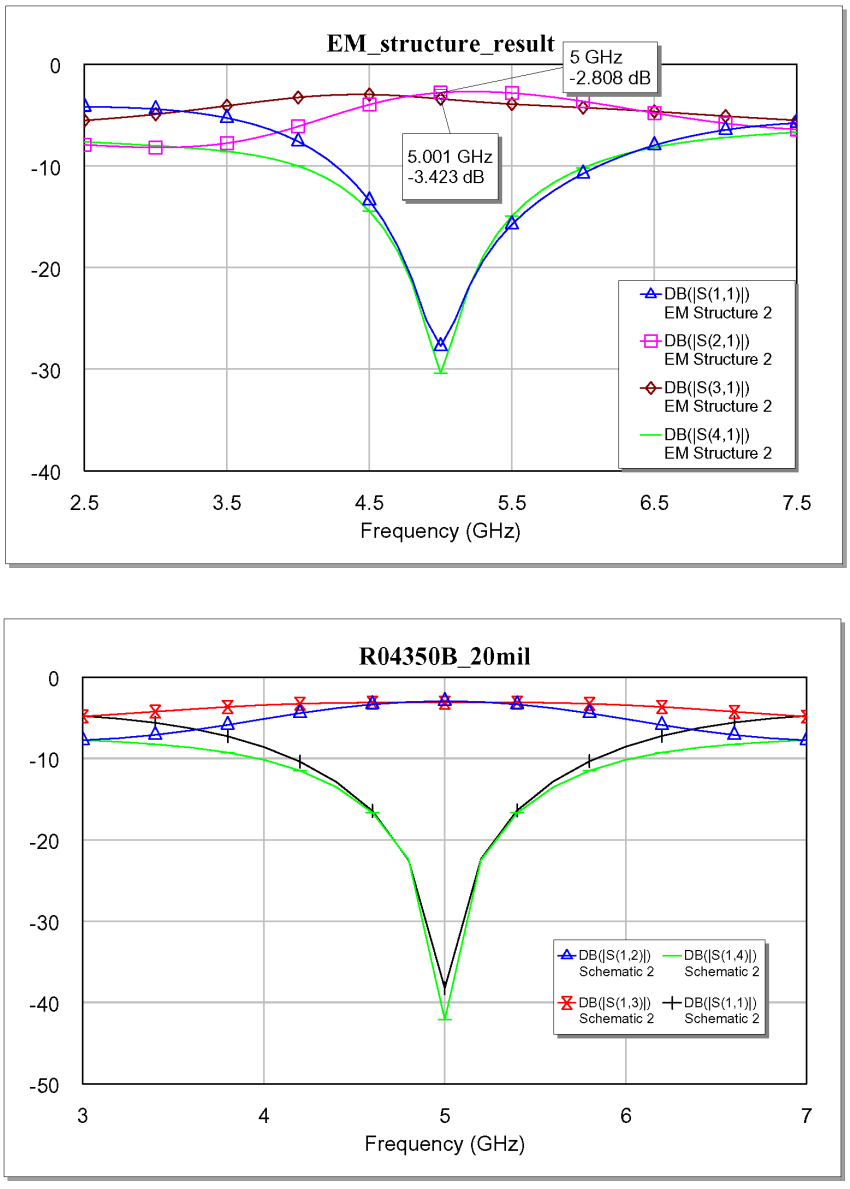

Fig. 5.1: y axis: S parameters in dB, top: Em structure simulation, dielectric material: RO4350B height 20mil, 50 Ω line: length 8870 μm, width: 1090μm, 35,35 Ω line: length 8650 μm, width: 1875 μm. bottom: Schematic simulation, same geometry of the transmission lines as for the Em structure simulation.

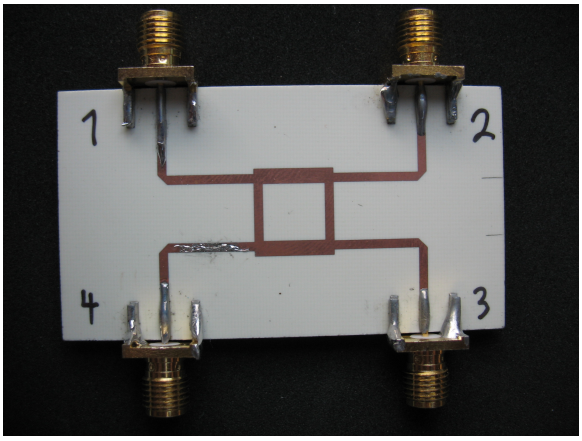

Fig. 5.2: Photo of the microstrip version of the 90° hybrid, design data: dielectric material: RO4350B height 20mil, 50 Ω line: length 8900 μm, width: 1100μm, 35,35 Ω line: length 8700 μm, width: 1900 μm.

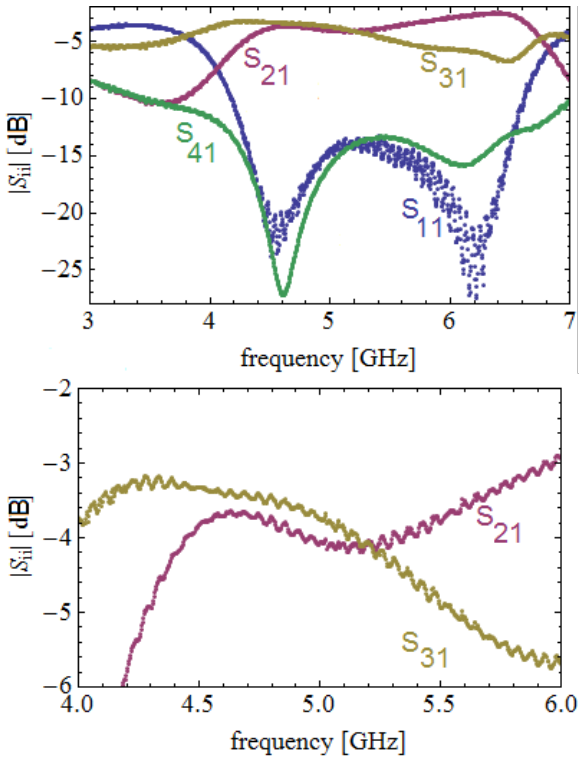

Fig. 5.3: Results of the microstrip version, bottom zoom in of upper graph

and as dielectric substrate Ad1000 is chosen with a height of 59mil. Due to the corners there are differences between the two results. The problem doing EM structure simulation was that simulating a CPW version of the beam splitter took about 5 hours. So this wasn't an efficient way to learn the behavior of the system when e.g. changing the geometry of corners.
The design corresponding to figure 5.6 was fabricated on a PC board, its design data are the same as for the corresponding simulation, see 5.6.

To measure this sample two runs were performed. In the first run the center ground was not connected to the other ground planes. So the part in the middle hadn't a fixed potential. The aim was to understand what this ungrounded plane would do. The outcome of the measurement is shown in figure 5.7. The parameters for S_{21} and S_{41} show the characteristic behavior like in the simulation. The matching of port one is not as pronounced as we hoped it would be. For S_{31} the result shows no similarity with simulated graph, the transmission to port 3 is far of from $-3\,\mathrm{dB}$. Reasons for this deviation could be due to the ungrounded center island.
To obtain the information whether the circuit is symmetric as it should be regarding the structure the S_{ii} parameters for the reflected waves were measured at each port when taken as input port. The outcome is displayed in figure 5.8. The lines don't lie on top of each other, so the structure is not symmetric. There might be two reasons for this: The first one is that the connection of the connectors to the board isn't perfect for each one. The second possibility to explain this is that the etching of the gap isn't symmetric. As mentioned in section 4.4.1 the photo resist is sprayed on the PC board by hand, so it won't have the same thickness overall the board. So the etch might cause to large gaps at sites where the nearby thickness of the photo resistor is smaller than in the case where it's thicker.
In addition as the gap size at the rims is larger, so that the connectors can be soldered on, in contrast to the gaps used for the rest of the circuit, the small gaps were free of copper earlier than the bigger ones. Thus the etching time for the small gaps was too long and therefore they are larger than wanted. This changes the impedance of the lines and therefore the system might not have the characteristic behavior as calculated in section 3.3. To quantify the possible error caused by variations of Z_0 and $\frac{Z_0}{\sqrt{2}}$ calculations as well as simulations will be performed.

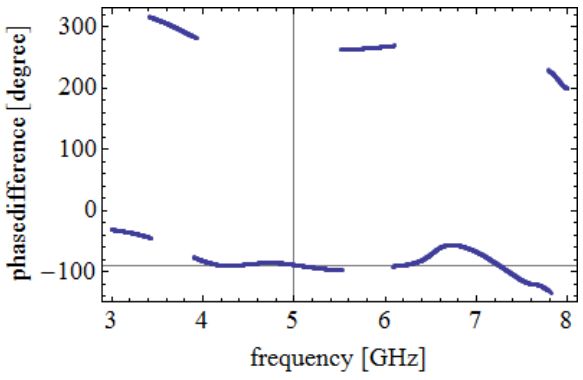

Fig. 5.4: Phase difference of microstrip version

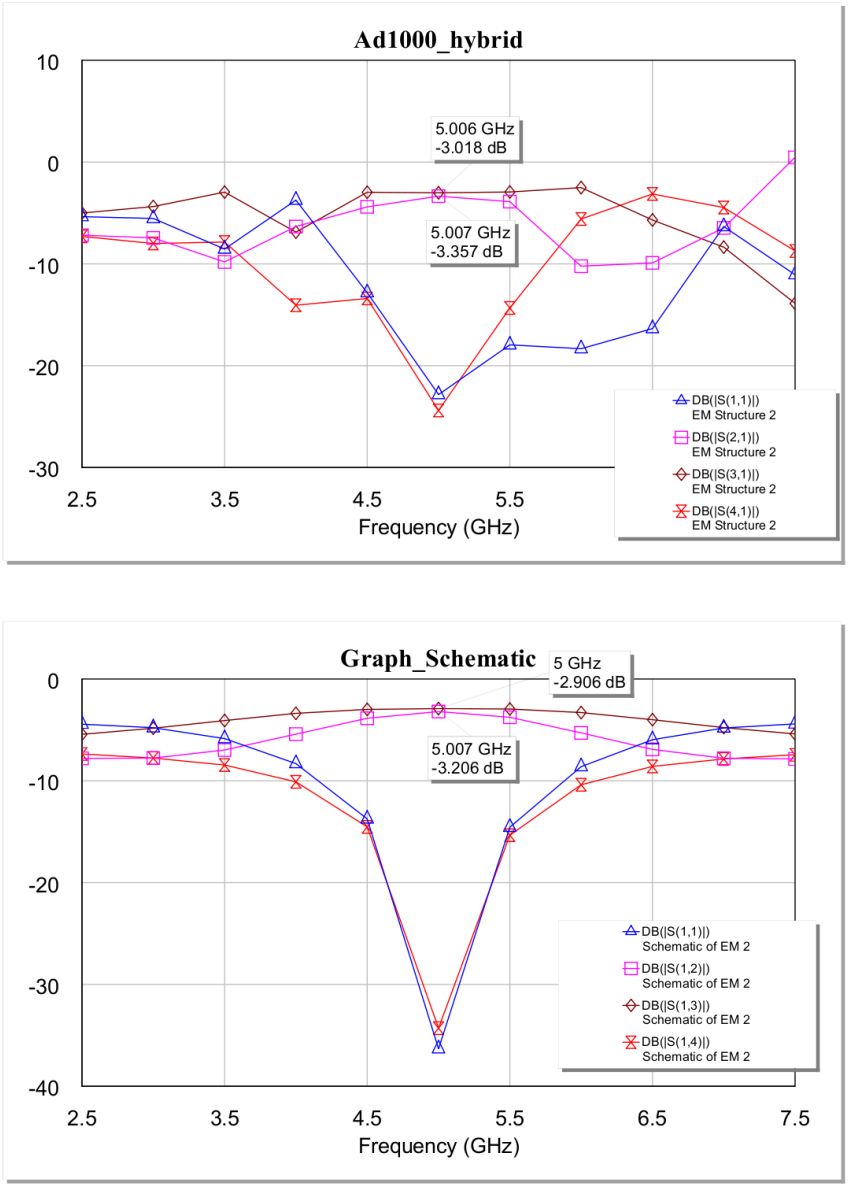

Fig. 5.5: Y-axis: S parameters in dB, top em structure simulation design data: dielectric: Ad1000 height 59 mil, design frequency 5 GHz, gap 400 μm, 50 Ω transmission line: length: 6400 μm, width: 700 μm, 35,35 Ω transmission line: length: 6200 μm, width: 1700 μm , bottom schematic simulation of coplanar waveguide version, same values for the geometry chosen as for em structure simulation.

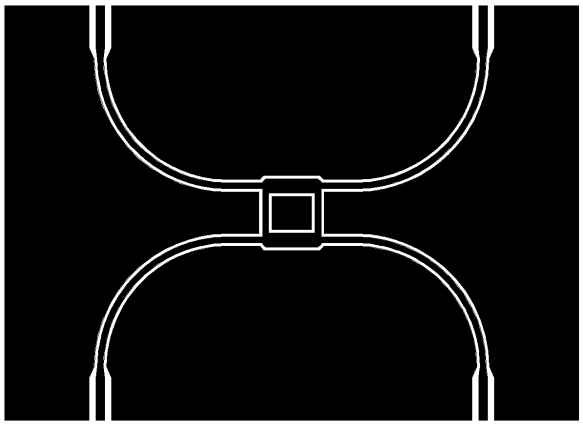

Fig. 5.6: Hybrid design on PC board Ad1000, design data: dielectric: Ad1000 height 59 mil, design frequency 5 GHz, gap 400 μm, 50 Ω transmission line: length: 6400 μm, width: 700 μm, 35,35 Ω transmission line: length: 6200 μm, width: 1700 μm.

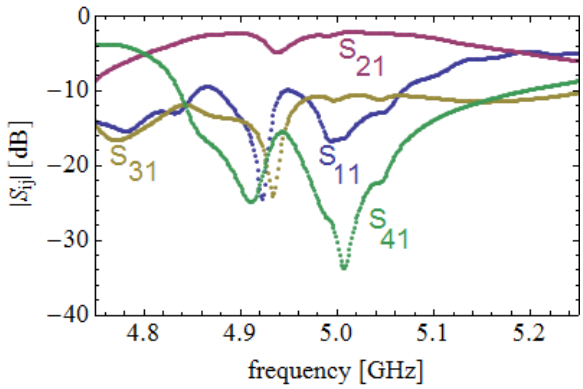

Fig. 5.7: CPW design, center isle not bonded, applied frequency versus S parameters of individual ports, design frequency 5 GHz

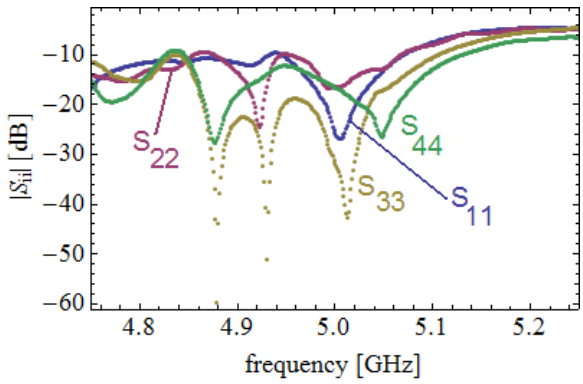

Fig. 5.8: Reflection matrix coefficients at the different ports

The phase difference of the output ports is plotted in figure 5.9. The phase is varying strongly around the design frequency.

We hoped to get an improvement if we connect the center ground to the lateral ground plane. This was done using 5 bond wires to each surrounding ground plane. Figure 5.10 and 5.11 show the obtained measured results where the top part in Fig. 5.10 is a detailed display of the S parameter values in the region near the design frequency.

Regarding the Fig 5.10 one can see that the graph deviates strongly from Fig. 3.8 where the calculated results are plotted. This was unexpected. The difference to the first measurements, see Fig. 5.7, is that the center is grounded which is expected to improve the result. But the result deviates much more stronger from the simulations a possible explanation is that there might be some coupling between the bond wires and the transmission lines. At least we measure a phase difference of 90° between the two output ports see figure 5.11. Actually the difference is 270° in the diagram due to the way the difference between the phases is calculated but corresponds but equals to a shift of 90° because 360°-270° = 90°.
Another possible reason why the CPW version isn't working well might be related to the chosen geometry of the circuit. As can be seen in Fig. 5.6 the size of the middle square is only around twice the size of the transmission lines. So there might be some coupling between the parallel transmission lines and they actually can't be treated as being independent as it was done in calculations.
A possibility to make further investigations would be to purchase a better simulation program which does a full three dimensional electromagnetic simulation of our design. Perhaps in this way the odd measured results could be explained due to some unwanted coupling between the transmission lines.
The current state of the project is that the CP-waveguide version doesn't work. Nevertheless there are several possibilities to proceed. The connection of the center isle could be done by a via through the board and a small connection cable soldered in to prevent the coupling of the bondwires. To get to know whether the connectors are the problem or the design itself, a simple transmission line could be fabricated and the reflection and transmission coefficients could be measured. Comparing the calculated result for the transmission with the measured one the quality of the connection could be obtained. Another possibility would be to create a

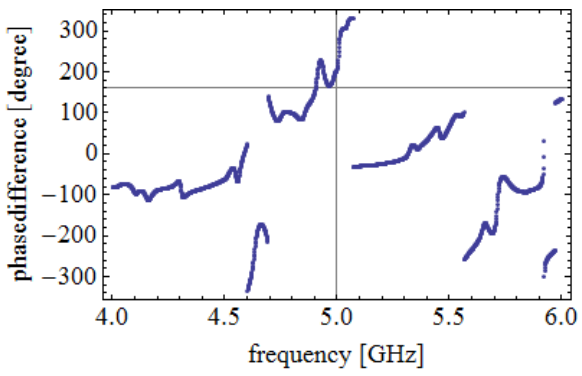

Fig. 5.9: Phase difference between the two output signals, center isle not bonded

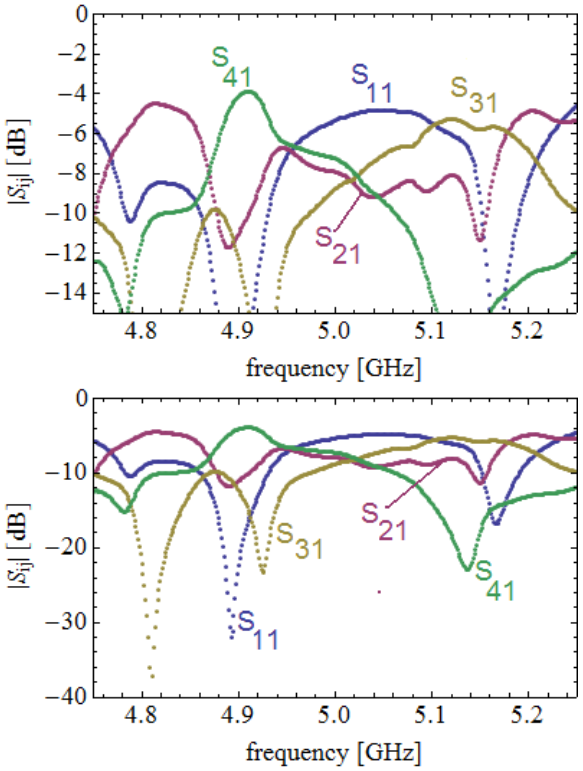

Fig. 5.10: Top: Detailed display of the S parameter values in the region near the design frequency of the bottom part, bottom: results bonded case in CPW technology, applied frequency versus S parameters of individual ports, design frequency 5 GHz.

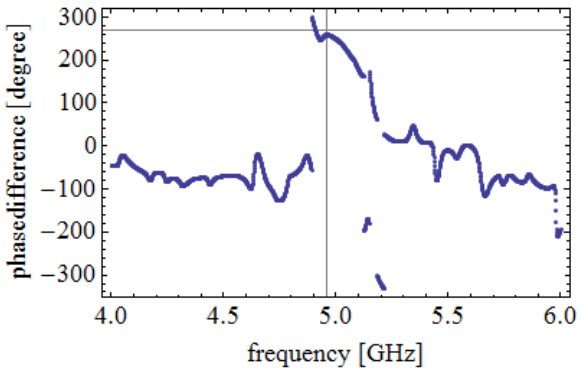

Fig. 5.11: Phase difference between the output ports 2 and 3 in the bonded case

design for a lower frequency, e.g. 500 MHz. For lower frequencies the not optimal connections wouldn't cause so big errors and the working of the design could be investigated. The problem in this case would be that the lines get longer, so the size of the simulation files would increase and simulation would take even longer than it takes now. But the advantage of the longer transmission lines would be that we have a larger ground plane in the middle and so coupling between the transmission lines would be very weak. So the transmission lines should behave like in theory where they are treated as one dimensional systems.

5.4 Superconducting CPW- circuits

As in the microstrip version as well as for the coplanar waveguide version the simulation of the em structure differed from the schematic due to the influence of the corners. Therefore simulations of different types of corners were performed in order to check their influence on the design for the superconducting circuit. As in the superconducting case the lines are quite small 10 μm for the 50 Ω and 25 μm for the 35,35 Ω line, the influence of the corner couldn't be recognized in the simulations, there was no difference between the different results detectable. In order to fit the design on a chip of the size of 2 mm by 7 mm size the values of 10 μm and 25 μm for the transmission lines were chosen. The 35,35 Ω line has a length so that it could be placed on the chip design without being curled. The 50 Ω had to be curled in order to be able realize the whole design on the given chip size. If possible on always curls the smaller transmission lines because the radius, you can curl your line with, without causing some unwanted reflection, increases with the width of your line. So by choosing the values of 10 μm for the 50 Ω and 25 μm for the 35,35 Ω line, the design shown in figure 5.12 could be developed. Designs were calculated and realized for design frequencies of 7, 8 and 9 GHz.
The advantage compared to the CPW PCB board model is that the transmission lines are longer and therefore have a larger ground plane in the middle. Therefore the coupling between the transmission lines should be weak and the transmission lines should show the behavior of a one dimensional system. Due to the superconducting phase a reduce in loss is expected and therefore a better agreement with the calculated values with an equal splitting of the input signal, with respect to power, to the output port should be found.

We had some problems in fabricating the designs. Therefore the measurements of the designs will be performed by the next semester student. His first measurement results of my samples are promising as the measurement values only deviate slightly from the calculated results. The reason and the quantization for this small deviations will be part of his thesis.

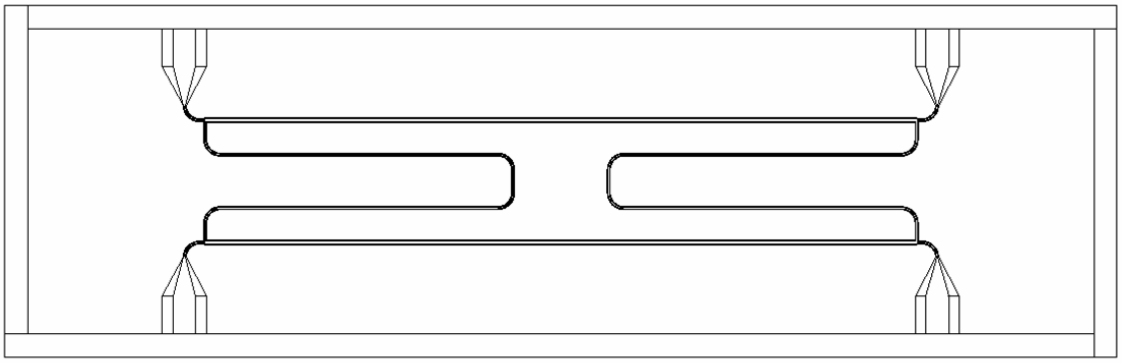

Fig. 5.12: Design of a 90° phase shift hybrid for a design frequency of 7 GHz, design data: dielectric sapphire, 50 Ω transmission line, bended lines in the diagram: length: 4670 μm width: 10 μm, gap between transmission line and ground: 4,5 μm. 35,35 Ω transmission line, horizontal line in the diagram: length: 4670 μm width: 24 μm, gap between transmission line and ground: 3 μm

6 Conclusion and Prospects

During this semester it was possible to get an understanding of the working principle of different types of circuit implementations of beam splitters. The most frequently used beam splitters were considered. For the 90° quadrature hybrid the calculations of its microwave properties were done in detail. For our purpose this is the most suitable design since it can be easily miniaturized and can be operated in the superconducting regime which gives the possibility to have a beam splitter with low loss. This is crucial for single photon correlation measurements where beam splitters are needed.
With microstrip circuits it was possible to show that the splitter is working in principle. The disadvantage of the mircostrip technology is that the width of the transmission lines is rather large. The width of the lines depends on the desired impedance, the dielectric constant and the thickness of the dielectric. So with this kind of realization it was not possible to fit the design on a chip of the size of 2 mm by 7 mm. This is the standard chip size used in our group and tools in order to measure the chip are designed for this size of the chip.
As CPW technology offers the possibility to shrink the size of the design by varying the gap between the transmission lines and the ground planes, designs and fabrication of CPW circuits on PC boards were achieved. The measured data strongly deviated from the simulated and calculated results. Possible reasons include that there might be coupling of the bond wires with the transmission lines and that the grounding of the center isle is not perfect. In addition the small size of the center isle compared to the width of the transmission line might allow some unwanted coupling between the transmission lines but results are not conclusive. The measurement of the superconducting circuits is still in progress, but first measurements of the superconducting samples which were performed recently are promising and only deviate slightly from the calculated values. The reason for this small deviations and its quantization will be addressed in the next thesis.

In order to improve the understanding of the CPW circuits on PC boards further steps could be done. To get a properly working beam splitter and to stop the coupling of the bond wires to the transmission lines one could make a little hole through the center isle and connect it via a short cable to the ground plane on the backside of the board. Like this one wouldn't have the bond wires going above the transmission lines and coupling could be prevented.
To investigate the role of the connectors and to estimate the loss of the transmission lines on a PC board, another step that should be done is fabricating a simple transmission line, solder two connectors on the board and measure the transmission and reflection coefficients. Like this one would know whether the CP- design didn't work or whether there are problems concerning the connectors and the loss.

As for high frequency signals the impedance matching is important in order to suppress reflections of the signal at impedance mismatches, a third possibility to proceed would be to design a circuit for a lower frequency e.g. 500 MHz. Errors occurring due to bad connection wouldn't be so critical at lower frequencies.

7 Appendix

7.1 Fabrication process for CPW circuits on a PCB

After the components of the design were assembled in a CAD program in the wanted way the parts where the metal shouldn't be etched away had to be colored. The next step was to add a reference strip of a known length below the design. This strip is needed when we transferred the design on a transparency later. Then the design was printed with a suitable scale, e.g. we did 2:1, so the printed version was double the size it should have later. After that the task was to transfer the design onto a transparency. To do so the printed version was put into an optical machine which consists of lenses which can be moved. In addition it was also possible to move the layer the printed version lies on in the machine. On top of the machine there was a glass plate on which was a half transparent paper mounted to see the projection of the circuit on. Next we moved the lenses and/or our object layer till we could see the circuit having the right size and being in focus on the half transparent piece of paper. To get the right size the already mentioned reference strip was necessary. As we knew the length of it we changed the position of the lenses and the object layer and measured then with a ruler the length this strip had on the half-transparent sheet. Having managed to have the right size and being in focus a photo detector was taken the exposure time can be obtained with. Then the exposure time was set on the machine, a piece of photo paper was put on the glass plate under the have transparent sheet, the lid covering the glass plate was closed and the vacuum pump was started. The vacuum was needed that the photo paper was pressed to the glass plate and wasn't wavy or something like that. After having exposed the photographic paper we put a transparency on top of it and put it in a second machine where it was developed. When the pair of transparency and photo paper came out of the machine we had to wait for another 75 seconds till the transparency was removed from the photo paper. Afterwards the transparency had to be cleaned in a bucket of water until the surface of the transparency wasn't slimy any longer. Now one just had to put the transparency into a dryer and then it was ready. We had the problem that our photo paper was a bit overexposed, therefore the lines on the transparency were a little shiny and we had to start again the whole process. So in our experience it was better to take shorter exposure time than given by the photo-detector. The next step was to transfer the structure from the transparency onto the PC-board. At first the PC-board had to be cleaned with soap and water and after that dried with the air gun. Then we put our PCB on a piece of paper and sprayed photo resistor on it as smoothly as possible and quickly covered it by building a tent of an other piece of paper above it. Like that it was possible to prevent as many dust as possible from falling onto the device while the resist was drying. Now the PC board was left at room temperature for roughly 30 minutes and

afterwards baked in the oven for 15 minutes at 60° C . The oven had already the appropriate settings and nothing had to be changed on its settings. The exposure time for the ultraviolet light was set to 30 seconds. After having exposed the PC board we developed our circuits with standard developer. The development time was roughly 30 seconds. Next the PC board was rinsed with water from the tap and dried again by using the air gun. An important step now was to put tape on the back of the plane because we wanted to keep the ground plane. Then the sample was mounted in the etching tank. Etching took around 3 minutes but it isn't possible to give an exact number because it strongly depended on how fresh the etch was. So you had to check regularly whether the copper was already etched away properly. After the etching was done we rinsed the sample with acetone and get rid of the photo resistor in this way. Directly afterwards ethanol was used to clean of the remains of acetone and finally dried it with the air gun. The last step in the fabrication process was to solder the connectors on and afterwards it was checked with an ohm meter whether an unwanted connection between the ground plane and the transmission line with solder was created.

7.2 Mathematica file

Mathematica file of the hybrid design for an easier reproducibility of the calculations and the possibility to expand the program.

Bibliography

[1] Hanbury and Twiss. A test of a new type of stellar interferometer on sirius. *Nature*, (178):1046–1048, 1956.

[2] Hanbury and Twiss. Correlations between photons in two coherent beams of light. *Nature*, (177):27–32, 1956.

[3] Moerner Lounis. Single photons in demand from a single molecule at room temperature. *Nature*, (407):491–493, 2000.

[4] Gordon Baym. The physics of hanbury brown–twiss intensity interferometry: from stars to nuclear collisions. *ACTA Physica Polonica B*, 29(7), 1998.

[5] Julien Gabelli. *Mise en évidence de la coherence quantique des conducteurs en régime dynamique*. PhD thesis, Université Paris 6, 2006.

[6] Walther. *Was ist Licht?* C.H. Beck, 1999.

[7] M. Teich B Saleh. *Fundamentals of Photonics*. Wiley & Sons, 1991.

[8] Prof. Ursula Keller. *Quantenelektronik*, summer term 2007 edition.

[9] H.Romer. *Theoretical Optics- and Introduction*. John Wiley & Sons, 2005.

[10] Christopher C. Gerry and Peter L. Knight. *Introductory quantum optics*. Cambridge University Press, 2005.

[11] R. Loudon. *The Quantum Theory of Light*. Oxford University Press, 2000.

[12] David M. Pozar. *Microwave Engineering*. John Wiley & Sons, 2005.

[13] C.C. Chen, J.T. Kuo, M. Jiang, and A. Chin. A fully planar microstrip coupled-line coupler with a high coupling level. *Microwave and optical technology letters*, 46(2):170–172, 2005.

[14] Rainee N. Simons. *Coplanar waveguide circuits, components and systems*. Wiley-Interscience, 2001.